Electronic excited states of conjugated cyclic ketones and thioketones: A theoretical study

Luis Serrano-Andrés[a] and Rosendo Pou-Amérigo
Departamento de Química Física, Instituto de Ciencia Molecular, Universitat de València, Dr. Moliner 50, Burjassot, E-46100 Valencia, Spain

Markus P. Fülscher[b]
Department of Theoretical Chemistry, Lund University, Chemical Center, P.O.B. 124, S-221 00 Lund, Sweden

Antonio Carlos Borin
Universidade de São Paulo, Instituto de Química, Av. Prof. Lineu Prestes 748, 05508-900, São Paulo, S. P., Brazil

(Received 2 January 2002; accepted 12 April 2002)

Absorption spectra of a series of cyclic conjugated ketones and thioketones have been computed at the multiconfigurational second-order multistate perturbation level of theory, the CASSCF/MS-CASPT2 method. Excitation energies, transition dipole moments, oscillator strengths, and static dipole moments are reported and discussed for excited states with energies lower than $\approx 7-8$ eV. The main bands of the spectra have been assigned and characterized in most cases for the first time. The spectroscopy of the different systems is compared in detail. Thioketones in particular have low-energy and intense $\pi\pi^*$ transitions which suggest corresponding enhanced nonlinear molecular optical properties. Additionally, some of the methods used to estimate these properties from spectroscopic data have been considered in order to analyze the main contributions to the nonlinear optical properties. © *2002 American Institute of Physics.* [DOI: 10.1063/1.1482706]

I. INTRODUCTION

Cyclopropenes, fulvenes, and heptafulvenes are nonalternant, cross-conjugated cyclic hydrocarbons with a strong double bond fixation.[1] The nonbezenoid aromatic character of the three- and seven-membered ring systems and the antiaromatic character of the five-membered ring systems, as well as their high reactivity, have attracted a great deal of attention.[2] The specific conjugation structure in these molecules results also in unusual and interesting excited states structures. For instance, unlike other systems of similar size and nature, they are colored compounds. The absorption bands are the result of low lying $\pi\rightarrow\pi^*$ excitations.[3] The low-energy electronic transitions and the large changes of the dipolar moment upon excitation are responsible for the enhancement of the electric properties of these compounds as compared to analogous systems. Such changes as the extension of the π-electron conjugation or the substitution of the exocyclic atom from oxygen to sulfur may dramatically decrease the gap between the excited and the ground state while do not increase significantly the overall molecular size.[4,5] All these facts are important in the context of nonlinear optical (NLO) materials.[5,6] Once an accurate and comprehensive study of the excited states structure of such systems is available by means of the CASSCF/MS-CASPT2 methodology, we will additionally complement the study with an analysis of the relation of the NLO properties to the electronic excited states.

The present paper reports calculations on the electronic spectra of a series of cyclic unsaturated ketones and thioketones: cyclopropenone (C_3H_2O), cyclopentadienone (C_5H_4O), and cycloheptatrienone (known as tropone, C_7H_6O) and the corresponding thioketones: cyclopropenethione (C_3H_2S), cyclopentadienethione (C_5H_4S), and cycloheptatrienethione (thiotropone, C_7H_6S). A detailed analysis will be performed for the excited states of the three-membered rings, where the basic nature of the low-lying states can be understood. The modest size of all these molecules allows us to use a high-level-correlated method, the CASSCF/MS-CASPT2 approach,[7,8] to study the structure of their electronic states. Singlet and triplet excited states of both valence and Rydberg nature are included in the calculations together with several transition properties. The results will be discussed and compared with the spectra of the parent hydrocarbons. As a final step, the contribution of the excited states to the NLO properties of the compounds will be analyzed by using the sum-over-states (SOS) method, able to estimate qualitatively nonlinear optical properties from spectroscopic data (Fig. 1).

II. METHODS AND COMPUTATIONAL DETAILS

The ground state geometry of cyclopropenone, cyclopentadienone, cycloheptatrienone, cyclopropenethione, cyclopentadienethione, and cycloheptatrienethione were taken from a previous work.[5] The molecules are placed on the *yz*

[a]Author to whom correspondence should be addressed. Electronic mail: Luis.Serrano@uv.es
[b]Permanent address: Department of Clinical Chemistry, Malmö University Hospital, S-205 02 Malmö, Sweden.

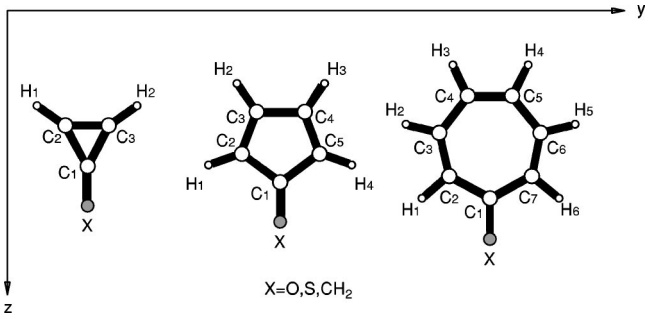

FIG. 1. Molecular structures, atom numbering, and definition of the axis system for the molecules discussed in the present work.

plane with the z axis as the C_2 symmetry axis (standard Mulliken orientation). At these geometries, the vertical excitation energies for all the systems were obtained with the CASSCF/multistate (MS) CASPT2 method,[9–11] using atomic natural (ANO) type basis sets[12,13] contracted to $5s4p2d$ functions for sulfur, $4s3p1d$ functions for carbon and oxygen, and $2s1p$ functions for hydrogen. A simultaneous description of both valence and Rydberg states is required for an accurate description of the spectra. Therefore an optimized set of $1s1p1d$ Rydberg-type functions, centered at the charge centroid of the molecule's cations was added to the atomic basis sets. The procedure employed to generate the Rydberg-type functions is described elsewhere.[14] A level shift of 0.30 hartree was used in the level-shift (LS) CASPT2 (Ref. 7) procedure after careful testing. While state energy differences were computed at the CASSCF, CASPT2, and MS-CASPT2 levels, transition dipole moments were obtained using the CAS state interaction (CASSI) method.[15] The state properties were computed using two different wave functions, CASSCF, and perturbatively-modified CAS-CI (PMCAS-CI).[10] The PMCAS-CI wave functions are built as linear combinations of the CASSCF wave functions with coefficients obtained from the quasidegenerated multistate perturbative treatment. These new wave functions have advantages in comparison with the CASSCF functions such as the diminished valence-Rydberg mixing. The basic characteristics of the PMCAS-CI functions have been described elsewhere.[10] For the sake of brevity just the PMCAS-CI properties and MS-CASPT2 (also CASSCF) excitation energies will be included into the tables. They are considered anyway the most accurate results.

To compute all excited states of interest, the active space should, in general, include valence $\pi\pi^*$ orbitals, high-lying lone pair orbitals, Rydberg orbitals of the first series (nine spd orbitals), and, eventually, valence $\sigma\sigma^*$ orbitals to check for the presence of states involving these orbitals, although they give rise usually to weak transitions. However, in order to avoid excessively large active spaces or to deal with intruder state problems, different active spaces were employed for states of different character and different molecules, always testing for the stability of the wave function. Within the C_{2v} symmetry, the notation $(a_1b_1b_2a_2)$ will be used for the description of the number of active orbitals used in the studied compounds. To compute the vertically excited states of cyclopropenone of A_1 and A_2 symmetry we used a (0641) active space, while for states of the B_1 and B_2 symmetries a space (6312) was employed. In C_3H_2S we used a (4531) active space in all the cases. Those active spaces included six electrons and at least nine Rydberg orbitals. Pilot calculations with extended active spaces designed to enable the description of $\sigma\sigma^*$ excitations were also performed. However, no such states were found at energies below 7.5 eV. The active spaces used to compute excited states of the five-ring systems included 12 electrons and 13 orbitals (3532). The latter included the valence π space, the lone pair of the heteroatom, two additional σ orbitals, and the four sp Rydberg orbitals. The equivalent active space, excluding the two additional σ orbitals, was used for the seven ring molecules, which consists of ten electrons and (2623) orbitals. All the energy differences were computed with respect to the ground state obtained with the same active space. The core orbitals ($1s$ for oxygen and carbon, $1s2s2p$ for sulfur) and electrons were frozen at the HF-SCF level of calculation and were not included at the correlated level. The calculations were performed with the MOLCAS-4.1 (Ref. 16) programs package.

TABLE I. Computed CASSCF (CAS), PMCAS-CI, and MS-CASPT2 (MSPT2) excitation energies (eV), oscillator strengths (f), orbital extensions ($\langle r^2\rangle$, a.u.), and dipole moments (μ, D) of the excited states and electronic transitions of the cyclopropenone (C_3H_2O) molecule.

			PMCAS-CI[a]		
State	CAS	MSPT2	f	$\langle r^2\rangle$	μ
$3\ ^1B_2$				46	−4.863
$2\ ^1A_1(n\rightarrow\pi^*)$	6.73	4.25	0.001	47	−0.522
$3\ ^1A_1(n\rightarrow\pi^*)$	5.93	5.59	forb.	46	−2.433
$2\ ^1A_2(\pi\rightarrow\pi^*)$	7.99	5.96	0.116	48	−1.925
$2\ ^1B_1(n\rightarrow 3s)$	7.83	6.90	0.018	108	9.502
$4\ ^1B_2(n\rightarrow 3p_z)$	8.24	7.24	0.012	82	−6.125
$5\ ^1B_2(n\rightarrow 3p_y)$	6.72	7.28	0.034	103	1.787
$3\ ^1B_1(\pi\rightarrow\pi^*)$	11.44	7.80	0.653	53	−4.032
$4\ ^1A_1(n\rightarrow 3p_x)$	7.02	7.88	forb.	150	−0.564
$3\ ^1A_2(n\rightarrow 3d_{xy})$	8.94	8.09	0.001	263	−11.870
$5\ ^1B_2(n\rightarrow 3d_{x^2-y^2})$	8.66	8.09	0.000	258	−7.634
$4\ ^1B_2(n\rightarrow 3d_{z^2})$	8.80	8.26	0.004	277	−6.612
$2\ ^1B_1(\pi\rightarrow 3s)$	8.59	8.30	0.011	101	7.545
$3\ ^1A_1(n\rightarrow 3d_{yz})$	7.49	8.30	0.008	307	−1.194
$3\ ^1A_2(n\rightarrow 3d_{xz})$	7.47	8.50	forb.	368	−5.718
$1\ ^3B_1(n\rightarrow\pi^*)$	5.61	4.05	⋯	48	−0.718
$1\ ^3B_2(\pi\rightarrow\pi^*)$	5.27	4.81	⋯	47	−3.385
$1\ ^3A_2(n\rightarrow\pi^*)$	4.31	5.56	⋯	44	−2.101
$1\ ^3A_1(\pi\rightarrow\pi^*)$	5.38	6.98	⋯	46	−2.274

[a]PMCAS-CI wave functions. See Methods.

III. RESULTS AND DISCUSSION

A. The spectra of cyclopropenone and cyclopropenethione

Tables I and II compile the computed excitation energies, oscillator strengths, orbital extensions, and dipole moment values for the states and transitions in the absorption spectra of C_3H_2O and C_3H_2S at different levels of approximation with respect to the treatment of the electronic correlation. The PMCAS-CI/MS-CASPT2 values will be consid-

TABLE II. Computed CASSCF (CAS), PMCAS-CI, and MS-CASPT2 (MSPT2) excitation energies (eV), oscillator strengths (f), orbital extensions ($\langle r^2 \rangle$, a.u.), and dipole moments (μ, D) of the excited states and electronic transitions of the cyclopropenethione (C_3H_2S) molecule.

			PMCAS-CI[a]		
State	CAS	MSPT2	f	$\langle r^2 \rangle$	μ
$1\,^1A_1$				62	−5.028
$1\,^1A_2(n\rightarrow\pi^*)$	3.89	3.23	forb.	62	−2.880
$1\,^1B_1(n\rightarrow\pi^*)$	4.62	3.47	0.000	64	0.413
$1\,^1B_2(\pi\rightarrow\pi^*)$	5.29	4.34	0.028	66	−0.551
$2\,^1B_2(n\rightarrow 3s)$	5.21	4.98	0.061	109	−0.701
$2\,^1A_1(\pi\rightarrow\pi^*)$	6.16	5.52	0.533	82	−4.540
$3\,^1B_2(n\rightarrow 3p_z)$	5.80	5.88	0.012	147	−1.757
$2\,^1A_2(n\rightarrow 3p_x)$	5.75	5.93	forb.	143	−1.415
$3\,^1A_1(n\rightarrow 3p_y)$	5.65	5.98	0.136	132	−0.909
$2\,^1B_1(\pi\rightarrow 3s)$	6.06	6.34	0.007	119	0.636
$4\,^1B_2(n\rightarrow 3d_{z^2})$	6.30	6.36	0.000	187	−16.973
$3\,^1A_2(n\rightarrow 3d_{xz})$	6.37	6.65	forb.	235	−16.332
$5\,^1B_2(n\rightarrow 3d_{x^2-y^2})$	6.46	6.71	0.026	244	−8.526
$4\,^1A_1(n\rightarrow 3d_{yz})$	6.45	6.78	0.061	226	−15.926
$3\,^1B_1(n\rightarrow 3d_{xy})$	6.55	6.79	0.024	247	−9.233
$4\,^1A_2(\pi\rightarrow 3p_y)$	6.50	6.91	forb.	140	−0.173
$4\,^1B_1(\pi\rightarrow 3p_z)$	6.68	6.99	0.041	141	−2.336
$5\,^1A_1(\pi\rightarrow 3p_x)$	7.57	7.10	0.075	139	−2.042
$5\,^1B_1(\pi\rightarrow 3d_{z^2})$	7.24	7.57	0.000	181	−20.919
$6\,^1A_1(\pi\rightarrow 3d_{xz})$	7.23	7.76	0.001	237	−19.296
$5\,^1A_2(\pi\rightarrow 3d_{yz})$	7.34	7.78	forb.	198	−17.264
$6\,^1B_1(\pi\rightarrow 3d_{x^2-y^2})$	7.34	7.85	0.005	236	−10.132
$6\,^1B_2(\pi\rightarrow 3d_{xy})$	7.62	7.92	0.009	246	−9.901
$1\,^3A_2(n\rightarrow\pi^*)$	3.43	3.20	⋯	61	−2.553
$1\,^3B_1(n\rightarrow\pi^*)$	3.78	3.30	⋯	65	0.356
$1\,^3B_2(\pi\rightarrow\pi^*)$	3.60	3.86	⋯	66	−1.806
$1\,^3A_1(\pi\rightarrow\pi^*)$	3.87	3.99	⋯	63	−2.770

[a]PMCAS-CI wave functions. See Methods.

ered as the final results to discuss the absorption spectra of the computed systems. Other values at the CASSCF/CASPT2 level can be found elsewhere.[17]

If we focus on PMCAS-CI/MS-CASPT2 values, the spectra of C_3H_2O and C_3H_2S both start with two low-lying and weak $n\rightarrow\pi^*$ transitions. In C_3H_2O the lowest excitation corresponds to the $1\,^1B_1$ state and can be interpreted as resulting from a one-electron promotion from the oxygen lone pair orbital of b_2 symmetry into the antibonding a_2 π^* orbital perpendicular to the C–O bond. There is therefore an important transfer of charge from the exocyclic heteroatom to the ring. This leads to a reduction of the polarity as reflected in the drastic decrease of the dipole moment from the ground state (−4.863 D) to the $1\,^1B_1$ state (−0.522 D). The second transition ($1\,^1A_2$) is also of $n\rightarrow\pi^*$ character, placed at 5.59 eV, and one-photon symmetry forbidden. It corresponds to the promotion of one electron from the oxygen lone pair to an orbital characterized as an antibonding π^* C═O orbital of b_1 symmetry. We find a concomitant decrease in the dipole moment of the $1\,^1A_2$ state as compared to the ground state value. However, the transfer of charge to the π system is in this case rather small. The reported electron impact spectrum of cyclopropenone[18] has two weak and structureless features with maxima at 4.13 and 5.5 eV, respectively. If we normalize the most intense peak of the spectrum at 7.8–8.1 eV to a relative intensity of 0.65, the corresponding values for the 4.13 and 5.5 eV bands would be 0.005 and 0.03, respectively. The band at 4.13 eV has been assigned to an $n\rightarrow\pi^*$ transition. In contrast, the 5.5 eV band was assumed to involve excitations from the σ bonds. This assignment seems unlikely because of the, in general, very small oscillator strength of $\sigma\rightarrow\pi^*$ transitions. On the basis of the present results we assign both bands to $n\rightarrow\pi^*$ transitions. The observed intensity for the 5.5 eV band is probably originated by borrowing intensity from higher bands. The described situation is similar in the C_3H_2S molecule although it has important differences: The first two transitions are of $n\rightarrow\pi^*$ type, but they are found at much lower energies than in C_3H_2O. In addition, the order of the states is reversed. The $1\,^1A_2$ state is computed to lie at 3.23 eV while the $1\,^1B_1$ state is located at 3.47 eV. The magnitude of the changes in the dipole moments upon excitation is similar to that observed in C_3H_2O, although in C_3H_2S the dipole moment of the $1\,^1B_1$ state changes the sign. The fact that the $1\,^1A_2$ state becomes lower in energy in C_3H_2S is clearly related to the nature of the C–S bond as compared with the C–O bond. The lengths of the C–S and C–O bonds are 1.617 Å and 1.214 Å, respectively, and, therefore, the excitation to the antibonding orbital localized at the C–S bond is lower in energy as compared to the situation in C_3H_2O.

Two $\pi\rightarrow\pi^*$ transitions correspond to the most intense bands in the computed absorption spectrum of C_3H_2O. The $1\,^1B_2$ state gives rise to a band at 5.96 eV with an oscillator strength of 0.116. At the PMCAS-CI level the wave function is clearly composed of a single configuration which represents an excitation from the $3b_1$ orbital (delocalized over the C═C bond and the oxygen atom) towards the $1a_2$ orbital (antibonding C═C orbital). The dipole moment of the $1\,^1B_2$ state is drastically reduced as compared to the ground state. The second $\pi\rightarrow\pi^*$ excitation, related to the $4\,^1A_1$ state, is computed to lie 7.80 eV above the ground state. It has an oscillator strength of 0.653 and the corresponding state dipole moment (−4.032 D) is close to the ground state value (−4.863 D). The state CASSCF wave function has a large multiconfigurational character. The main contribution can be mainly attributed to an excitation from the same $3b_1$ orbital to the $4b_1$ orbital. The latter is a π^* orbital delocalized over the entire molecule (carbons and oxygen) and explains the small change in dipole moments as compared to the ground state. The computed results correlate quite well with the electron impact spectrum of cyclopropenone.[18] A valence $\pi\rightarrow\pi^*$ transition of medium intensity was reported at 6.1 eV (relative intensity 0.20), corresponding to the transition towards the $1\,^1B_2$ state. A second band was found in the range from 7.9 to 8.2 eV with a sharp maximum at 8.1 eV.[18] In addition, there is a rich structure of Rydberg transitions which makes it difficult to accurately place the valence band. It is clear from the reported spectrum that the broad and intense band beneath the highest peaks must correspond to a valence excitation, which we assign to the $4\,^1A_1$ band. In C_3H_2S the two equivalent $\pi\rightarrow\pi^*$ transitions have lower energies in agreement with the larger size of the sulfur atom and longer C═S bond as compared to C_3H_2O. Here too, the $1\,^1B_2$ state remains the lowest of the two $\pi\rightarrow\pi^*$ excited states and the corresponding band is predicted to have a

maximum at 4.34 eV and an oscillator strength of 0.028. Thus, the $1\,^1B_2$ band is redshifted by 1.57 eV in comparison to C_3H_2O. The redshift for the second $\pi\rightarrow\pi^*$ excited transition ($2\,^1A_1$) is found to be even larger, 2.28 eV, placing the absorption maximum at 5.52 eV, with an oscillator strength of 0.533. The changes in the dipole moments are similar to those calculated for C_3H_2O.

Apart from the valence spectrum, a number of Rydberg transitions have been also computed. In C_3H_2O the first Rydberg series originates from excitations from the oxygen lone pair orbital. The lowest Rydberg excited state, the $2\,^1B_2$ $n\rightarrow 3s$ state, is predicted at 6.90 eV. The distinct diffuse character of the Rydberg states can be observed in the values of $\langle r^2\rangle$, which are much larger than for the valence states. Table I also includes one member of the second Rydberg series. This state originates from a one-electron promotion from the the highest b_1 π orbital and is placed at 8.30 eV. In C_3H_2S, the first Rydberg series starts with the $2\,^1B_2$ $n\rightarrow 3s$ transition at 4.98 eV and ends at 6.79 eV for C_3H_2O. Members of the second Rydberg series are found in the energy range from 6.34 eV (the $2\,^1B_1$ $\pi\rightarrow 3s$ state) to 7.92 eV. For both series the excitation energies decrease about 2 eV with respect to the corresponding states in C_3H_2O. With the exception of $3\,^1A_1$ $n\rightarrow 3p_y$ state, the computed oscillator strengths for the Rydberg transitions are very small. Unfortunately, comparison to experiment is almost impossible because, to the best of our knowledge, there is not enough information available. Comparing the spectroscopic properties of similar compounds, Harshbarger and co-workers[18] estimated the position of some Rydberg excited states: $n\rightarrow 3s$ at 6.22 eV, $n\rightarrow 3p$ at 6.88 eV, and $\pi\rightarrow 3s$ at 7.73 eV. On the basis of our results it seems that they systematically underestimated the position of the states by 0.6 eV. In addition, the observed spectrum displays the sharpest and most distinct Rydberg peaks between 6.9–7.2 eV and 7.9–8.3 eV, which are the regions where the calculations place the most intense of the Rydberg excitations.

A number of triplet states have been also computed. In C_3H_2O, the low-lying triplet excited valence state, the $1\,^3B_1$ ($n\rightarrow\pi^*$) state, is found to be located at 4.05 eV. Unlike for the singlet–singlet transitions, the second lowest excited state is not of the $n\rightarrow\pi^*$ nature. It originates in a $\pi\rightarrow\pi^*$ transition to the $1\,^3B_2$ state at 4.81 eV. In C_3H_2S the order in the triplet–triplet transitions remains the same as for their equivalent singlet–triplet states in C_3H_2O.

B. Comparison between CASSCF/CASPT2 and PMCAS-CI/MS-CASPT2 results

Because of significant state interaction matrix elements, the results obtained at the CASSCF/CASPT2 and the PMCAS-CI/MS-CASPT2 levels of approximation differ with respect to the properties of the individual states and transitions properties.[17] This is particularly true for the excitation energies to the $\pi\rightarrow\pi^*$ states, undergoing decreases of about 0.4–0.6 eV when changing from one to the other approach. Oscillator strengths and dipole moment values undergo somewhat smaller changes. The large and, in principle, unexpected differences, are mainly related to the extent of the valence-Rydberg mixing of the different states. The $n\rightarrow\pi^*$ states, for instance, are compact already at the CASSCF level, and have orbital extensions, $\langle r^2\rangle$, similar to those of the ground state. Therefore the difference in the transition energies calculated at the CASPT2 and the MS-CASPT2 level of approximation are always very small (only for the $1\,^1A_2$ $n\rightarrow\pi^*$ in C_3H_2O increases to 0.15 eV). Likewise the properties computed on the basis of the CASSCF wave functions are very similar to those derived from the PMCAS-CI wave functions. The latter are linear combination of the CASSCF wave functions of the states of the same symmetry which are included in the multistate treatment. The $\pi\rightarrow\pi^*$ states exhibit, however, a different behavior. For instance, the $2\,^1A_1$ state of C_3H_2S has a $\langle r^2\rangle$ of 132 a.u. at the CASSCF level, which closely resembles, and even exceeds, the extensions of some of the Rydberg states. The interaction of the $2\,^1A_1$ state with the other state of $^1A_1$ symmetry, especially with the $\pi\rightarrow pd$ Rydberg states, causes a drastic change in the character of the wave function, as well as a change in the excitation energies. The $2\,^1A_1$ state becomes much more compact at the PMCAS-CI level ($\langle r^2\rangle$ of 82 a.u.); the oscillator strength of the corresponding transition increases from 0.256 (CASSCF) to 0.533 (PMCAS-CI), and the dipole moment of the state slightly increases. It is clear that the $2\,^1A_1$ state has acquired much more valence character. On the other hand, the changes in the Rydberg states of $^1A_1$ symmetry are also noticeable: For almost all states the excitation energy remains almost unchanged as compared to the CASPT2 value except for the $6\,^1A_1$ ($\pi\rightarrow 3d_{xz}$) state which increases by 0.54 eV owing to the interaction with the valence state. The oscillator strength of the transitions decreases strongly for both the $5\,^1A_1$ ($\pi\rightarrow 3p_x$) and $6\,^1A_1$ ($\pi\rightarrow 3d_{xz}$) states, and the changes in the dipole moment values are also of significance. A similar situation is also observed for the other $\pi\rightarrow\pi^*$ states in C_3H_2O and C_3H_2S. The strength of the state interactions depends on many factors such as the degree of the near-degeneration and the basis sets used. Especially, the basis set dependency has been discussed earlier at several occasions.[10,19] It is therefore not surprising to find that calculations using different, in particular much smaller, basis sets may provide results computed at the CASPT2 level of theory which are in good agreement with results obtained using MS-CASPT2/PMCAS-CI approach in combination with large, flexible basis sets. The relevant values for the previous discussion can be found elsewhere.[17]

C. The spectra of cyclopentadienone and cyclopentadienethione

The spectra of the fulvene-type molecules have a number of important differences as compared to the three-ring systems which can be rationalized on the basis of their orbital structure. Unlike C_3H_2O and C_3H_2S, the HOMO orbital of the five-membered ring systems is a π orbital of a_2 symmetry, localized at the ring, and corresponds to the antisymmetric combination of ethene alike π orbitals. The LUMO is a π^* orbital of b_1 symmetry, very low in energy, and delocalized over the whole system. Therefore, $\pi\rightarrow\pi^*$ excitations of B_2 symmetry can be expected at low energies. In spite of that, the $n\rightarrow\pi^*$ $1\,^1A_2$ state is still found to be the

TABLE III. Computed CASSCF (CAS), PMCAS-CI, and MS-CASPT2 (MSPT2) excitation energies (eV), oscillator strengths (f), orbital extensions ($\langle r^2 \rangle$, a.u.), and dipole moments (μ, D) of the excited states and electronic transitions of the cyclopentadienone (C_5H_4O) molecule.

			PMCAS-CI[a]		
State[b]	CAS	MSPT2	f	$\langle r^2 \rangle$	μ
$1\,^1A_1$				71	−3.169
$1\,^1A_2(n\rightarrow\pi^*)$	4.71	2.48	forb.	70	−0.839
$1\,^1B_2(\pi\rightarrow\pi^*)$	6.66	3.00	0.045	62	−6.204
$1\,^1B_1(n\pi\rightarrow\pi^*\pi^*)$	6.65	4.49	0.000	64	−1.083
$2\,^1A_1(\pi\pi\rightarrow\pi^*\pi^*)$	6.02	5.42	0.097	71	−4.219
$3\,^1A_1(\pi\rightarrow\pi^*)$	7.77	5.98	0.259	74	−3.661
$2\,^1A_2(\pi\rightarrow 3s)$	7.90	6.50	forb.	120	1.444
$3\,^1A_2(n\rightarrow\pi^*)$	9.08	6.66	forb.	70	−1.912
$4\,^1A_2(\sigma\rightarrow\pi^*)$	9.48	6.81	forb.	85	−1.229
$2\,^1B_2(n\rightarrow 3s)$	8.21	6.87	0.015	126	−3.179
$4\,^1A_1(n\rightarrow 3p_y)$[c]	9.21	7.02	0.036	122	−3.154
$2\,^1B_1(\pi\rightarrow 3p_y)$	8.18	7.06	0.037	188	−1.738
$3\,^1B_2(\pi\pi\rightarrow\pi^*\pi^*)$	9.72	7.08	0.016	66	−1.829
$3\,^1B_1(n\rightarrow\pi^*)$	10.91	7.09	0.000	73	0.072
$5\,^1A_1(\pi\rightarrow\pi^*)$	10.84	7.10	0.384	77	−2.280
$5\,^1A_2(n\rightarrow 3p_x)$	8.62	7.11	forb.	115	−1.937
$4\,^1B_2(\pi\rightarrow 3p_x)$	8.30	7.16	0.025	144	−3.062
$6\,^1A_2(\pi\rightarrow 3p_z)$	8.55	7.19	forb.	125	−0.683
$5\,^1B_2(n\rightarrow 3p_z)$	8.65	7.32	0.008	121	−0.155
$1\,^3B_2(\pi\rightarrow\pi^*)$	2.38	1.97	⋯	75	−3.664
$1\,^3A_2(n\rightarrow\pi^*)$	3.54	2.51	⋯	71	−1.511
$1\,^3A_1(\pi\rightarrow\pi^*)$	2.90	3.78	⋯	77	−1.118
$1\,^3B_1(n\pi\rightarrow\pi^*\pi^*)$	5.63	4.46	⋯	73	−0.994

[a]PMCAS-CI wave functions. See Methods.
[b]Labels ($\pi\pi\rightarrow\pi^*\pi^*$) or ($n\pi\rightarrow\pi^*\pi^*$) describe states with predominant double excited character.
[c]Due to intruder state problems a level-shift of 0.4 a.u. was used in this state.

TABLE IV. Computed CASSCF (CAS), PMCAS-CI, and MS-CASPT2 (MSPT2) excitation energies (eV), oscillator strengths (f), orbital extensions ($\langle r^2 \rangle$, a.u.), and dipole moments (μ, D) of the excited states and electronic transitions of the cyclopentadienethione (C_5H_4S) molecule.

			PMCAS-CI[a]		
State[b]	CAS	MSPT2	f	$\langle r^2 \rangle$	μ
$1\,^1A_1$				90	−2.369
$1\,^1A_2(n\rightarrow\pi^*)$	2.67	1.43	forb.	88	−0.127
$1\,^1B_2(\pi\rightarrow\pi^*)$	4.04	1.99	0.002	82	−6.397
$1\,^1B_1(n\pi\rightarrow\pi^*\pi^*)$	3.95	2.89	0.000	82	−1.448
$2\,^1A_1(\pi\rightarrow\pi^*)$	5.99	4.42	0.368	91	−3.646
$3\,^1A_1(\pi\pi\rightarrow\pi^*\pi^*)$	5.60	4.84	0.000	88	−5.016
$4\,^1A_1(nn\rightarrow\pi^*\pi^*)$	6.86	5.06	0.050	88	1.327
$2\,^1A_2(n\pi\rightarrow\pi^*\pi^*)$	6.61	5.13	forb.	93	−1.167
$2\,^1B_2(\pi\rightarrow\pi^*)$	7.40	5.38	0.005	85	−5.560
$3\,^1A_2(\sigma\rightarrow\pi^*)$	7.66	5.73	forb.	100	−0.383
$3\,^1B_2(n\rightarrow 3s)$	6.45	5.84	0.065	154	−2.968
$2\,^1B_1(\sigma\rightarrow\pi^*)$	7.71	5.96	0.032	89	−1.475
$4\,^1A_2(\pi\rightarrow 3s)$	6.75	6.07	forb.	150	2.392
$5\,^1A_1(n\pi\rightarrow\pi^*\pi^*)$	7.29	6.11	0.000	104	−3.830
$5\,^1A_2(n\rightarrow\pi^*)$	9.27	6.19	forb.	89	−0.286
$6\,^1A_1(n\rightarrow 3p_y)$	6.51	6.30	0.001	225	−3.018
$4\,^1B_2(n\rightarrow 3p_z)$	6.99	6.33	0.006	149	−3.820
$6\,^1A_2(n\rightarrow 3p_x)$	7.04	6.36	forb.	169	−0.171
$3\,^1B_1(n\rightarrow\pi^*)$	9.17	6.59	0.000	89	1.193
$4\,^1B_1(\pi\rightarrow 3p_y)$	7.05	6.65	0.022	230	2.491
$5\,^1B_2(\pi\rightarrow 3p_x)$	7.10	6.71	0.025	179	0.357
$7\,^1A_2(\pi\rightarrow 3p_z)$	7.39	6.74	forb.	159	−0.081
$1\,^3A_2(n\rightarrow\pi^*)$	0.82	1.26	⋯	90	−0.319
$1\,^3B_2(\pi\rightarrow\pi^*)$	1.17	1.61	⋯	90	−3.776
$1\,^3A_1(\pi\rightarrow\pi^*)$	2.17	2.41	⋯	90	−1.934
$1\,^3B_1(n\pi\rightarrow\pi^*\pi^*)$	2.67	2.88	⋯	90	−1.707

[a]PMCAS-CI wave functions. See Methods.
[b]Labels ($\pi\pi\rightarrow\pi^*\pi^*$) or ($n\pi\rightarrow\pi^*\pi^*$) describe states with predominant double excited character.

lowest singlet-singlet excited valence state in the spectra of both C_5H_4O (2.48 eV) and C_5H_4S (1.43 eV). Here too, the decrease in the excitation energy upon replacement of the oxygen atom by sulfur is large and can be related to the length of the exocyclic heteroatomic bond (C═O 1.227 Å, C═S 1.633 Å). The second transition is, however, of $\pi\rightarrow\pi^*$ in origin. The corresponding $1\,^1B_2$ states are found at 3.00 and 1.99 eV, respectively. The intensity of these $\pi\rightarrow\pi^*$ transitions is not particularly high.

Another consequence of the small $\pi\rightarrow\pi^*$ orbital energy gap is to favor low-energy electronic states with strong multiconfigurational character and significant contributions from doubly or higher excited configurations. The analysis of the CASSCF wave functions for the $1\,^1B_1$ states of C_5H_4O and C_5H_4S reveals that these states have large contributions from double excitations. They are found at 4.49 and 2.89 eV, respectively. For this reason the character of these and similar states are labeled ($n\pi\rightarrow\pi^*\pi^*$) or ($\pi\pi\rightarrow\pi^*\pi^*$) in Tables III and IV.

Experimental spectroscopic information is sparse. The UV spectra reported by Garbisch *et al.*[20] display two bands at 3.27 and 6.21 eV for C_5H_4O with extinction coefficients 79 and 55 000 $l\,mol^{-1}\,cm^{-1}$, respectively. In view of our calculations the assignment is straightforward although there are certain deviations. Assuming that the experimentally observed transitions are of $\pi\rightarrow\pi^*$ character the bands should be assigned to the $1\,^1B_2$ and $3\,^1A_1$ states at 3.00 eV and 5.98, respectively. The deviation of calculated and experimental excitations energies is near 0.3 eV and larger than observed previously for many different systems. However, a comparison of the results obtained with the CASSCF/CASPT2 and the PMCAS-CI/MS-CASPT2 approaches shows that the CASPT2 wave function for the $\pi\rightarrow\pi^*$ excited states strongly interact with near degenerate states, leading possibly to less accurate results. We have not found any more recent and detailed experimental data concerning the spectrum of this molecule. The most intense bands of our theoretical spectrum correspond to transitions to the $3\,^1A_1$ state at 5.98 eV (oscillator strength 0.259) and $5\,^1A_1$ at 7.10 eV (0.384). The absence of the transition at 5.42 eV is somewhat surprising.

Comparing the Rydberg excited states in C_5H_4O with those of C_5H_4S (only the $3s$ and $3p$ components have been computed) we observe significant differences. In C_5H_4O the two lowest Rydberg series start at 6.50 and 6.87 eV, corresponding to the $\pi\rightarrow 3s$ ($2\,^1A_2$ state) and $n\rightarrow 3s$ ($3\,^1B_2$) transitions, respectively. In C_5H_4S, the equivalent transitions and state change order and decrease their energies in a very different way. Therefore, the $n\rightarrow 3s$ ($3\,^1B_2$) transition becomes the lowest Rydberg excitation at 5.84 eV while the $\pi\rightarrow 3s$ ($4\,^1A_2$) transition is located at 6.57 eV. The energy decrease with respect to C_5H_4O is 1.03 eV ($n\rightarrow 3s$) and 0.43 eV ($\pi\rightarrow 3s$), respectively. These trends, which can be re-

lated with the character of the carbon–sulfur bond, are a common characteristic of all the systems studied here once sulfur replaces oxygen.

Pilot calculations on C_5H_4O and C_5H_4S showed that, unlike the three-membered ring systems, the electronic spectra of the pentadieneketones have also $\sigma\rightarrow\pi^*$ transitions at very low energy. Therefore, we used an extended active space for the five-membered ring systems. The final results include for C_5H_4O one $\sigma\rightarrow\pi^*$ $4\,^1A_2$ excited state located at 6.81 eV and for C_5H_4S two $\sigma\rightarrow\pi^*$ excited states, $3\,^1A_2$ and $2\,^1B_1$, located at 5.73 and 5.96 eV, respectively. All these transitions are one-photon forbidden or, at least, have low intensity.

As regarding the triplet states, the effect of the low-lying $\pi\rightarrow\pi^*$ excitations can be also observed in their relative position. In C_5H_4O the $\pi\rightarrow\pi^*$ $1\,^3B_2$ state is the lowest one in the spectrum at 1.97 eV, followed by the $n\rightarrow\pi^*$ $1\,^3A_2$ state at 2.51 eV. In the sulfur compound their order is reversed: $1\,^3A_2$ at 1.26 eV and $1\,^3B_2$ at 1.61 eV.

D. The spectra of tropone and thiotropone

The orbital structure of the seven-ring compounds tropone (C_7H_6O) and thiotropone (C_7H_6S) changes from that of the five-ring fulvene-type systems. A b_1 π orbital becomes the HOMO orbital, while a pair of near-degenerate a_2 and b_1 π^* orbitals are the lowest-lying virtual valence orbitals. The orbitals of b_1 symmetry are typically delocalized in both the ring and the C═O or C═S moieties. In contrast, orbitals of a_2 symmetry are limited to the ring system. Both C_7H_6O and C_7H_6S molecules have two low-lying $n\rightarrow\pi^*$ states which are very close in energy (because of the closeness of the low-lying virtual a_2 and b_1 orbitals). The decrease in energies between the $n\rightarrow\pi^*$ states of tropone (3.86 and 3.94 eV) and thiotropone (2.05 and 2.10 eV) is much larger than in the other compounds. In order of ascending state energies next follow a pair of $\pi\rightarrow\pi^*$ excited valence states. They can be characterized to arise from excitations from the HOMO b_1 π orbital to the low-lying virtual a_2 and b_1 orbitals. The electronic singlet states with energies higher than the two lowest $\pi\rightarrow\pi^*$ excited valence states are typically composed of contributions of several configurations, that is, they have a clear multiconfigurational character. The labels used to characterize the states in Tables V and VI have been chosen such as to describe the largest contribution. Unlike the fulvene-type molecules, more detailed experimental information is available for the heptafulvene-type systems. Evidence for the presence of $n\rightarrow\pi^*$ transitions at low energies have been reported for several tropones. The most intense bands observed in the spectrum of tropone (C_7H_6O) in the vapor are: a medium intense transition at 4.13 eV, an intense peak at 5.56 eV (both having in-plane polarization), a broad shoulder at 6.9 eV, and an intense group of transitions above 7.2 eV. The latter have not been studied in detail.[21] The estimated oscillator strengths of the three low-energy features are 0.13, 0.37, and 0.1, respectively.[21] Studies on the polarization of the low-lying band in the vapor spectrum of C_7H_6O,[21,22] at 4.13 eV showed that it is composed of overlapping transitions of different polarization, perpendicular to the molecular plane ($n\rightarrow\pi^*$ type) and parallel to it ($\pi\rightarrow\pi^*$). The estimated oscillator strengths (if two bands were considered to form the 4.13 eV transition) are 0.01 and 0.12,[21] respectively. The calculated $n\rightarrow\pi^*$ transitions in tropone lie at 3.86 and 3.94 eV and can be clearly related to the observed out-of-plane transition, while the $\pi\rightarrow\pi^*$ transitions computed to the $2\,^1A_1$ and $1\,^1B_2$ states are obtained at 4.22 and 4.26 eV, with oscillator strengths 0.064 and 0.042, respectively. These four excitations originate the band observed at 4.13 eV with a small intensity. The band undergoes a slight redshift in polar solvents,[21] which can be related to the stabilization of the $2\,^1A_1$ state which has a large dipole moment. As regards the spectrum of C_7H_6S in hexane solution, a very weak band has been identified at 1.82 eV followed by another weak feature at 2.03 eV. Both were reported to have low extinction coefficients, 9 and 47 $\mathrm{l\,mol^{-1}\,cm^{-1}}$, respectively.[23] In the energy range close to 2 eV we have computed two states, $1\,^1A_2$ and $1\,^1B_1$. The $1\,^1A_2$ state may be related to the band at 1.82 eV, although the presence of a nearby excitation to a triplet state has to be noticed. It is, however, most likely that the 2.03 eV band arises from a mixture of an $n\rightarrow\pi^*$ excitation and the more intense $\pi\rightarrow\pi^*$ transition to the $1\,^1B_2$ state.

The computed data lead to a clear interpretation of the experimental observations also for the remaining data in both compounds. A $\pi\rightarrow\pi^*$ transition has been computed for

TABLE V. Computed CASSCF (CAS), PMCAS-CI, and MS-CASPT2 (MSPT2) excitation energies (eV), oscillator strengths (f), orbital extensions ($\langle r^2\rangle$, a.u.), and dipole moments (μ, D) of the excited states and electronic transitions of the cycloheptatrienone (C_7H_6O) molecule.

			PMCAS-CI[a]		
State[b]	CAS	MSPT2	f	$\langle r^2\rangle$	μ
$1\,^1A_1$				101	−3.741
$1\,^1B_1(n\rightarrow\pi^*)$	4.36	3.86	0.000	95	−0.416
$1\,^1A_2(n\rightarrow\pi^*)$	4.28	3.94	forb.	95	−1.252
$2\,^1A_1(\pi\pi\rightarrow\pi^*\pi^*)$	5.04	4.22	0.064	104	−4.241
$1\,^1B_2(\pi\rightarrow\pi^*)$	4.83	4.26	0.042	102	−3.648
$3\,^1A_1(\pi\rightarrow\pi^*)$	7.68	5.67	0.280	105	−4.526
$2\,^1B_2(\pi\rightarrow\pi^*)$[c]	5.95	6.05	0.012	100	−2.613
$2\,^1B_1(\pi\rightarrow 3s)$	5.76	6.19	0.000	162	3.474
$3\,^1B_2(\pi\rightarrow\pi^*)$	7.23	6.31	0.055	108	−3.621
$4\,^1B_2(n\rightarrow 3s)$	6.31	6.74	0.003	155	1.127
$2\,^1A_2(\pi\rightarrow 3p_y)$	6.29	6.81	forb.	202	1.122
$4\,^1A_1(\pi\rightarrow 3p_x)$	6.40	6.97	0.005	197	2.066
$3\,^1B_1(\pi\rightarrow 3p_z)$	6.46	7.02	0.015	202	−2.466
$5\,^1A_1(\pi\rightarrow\pi^*)$	7.45	7.05	0.000	121	−2.887
$6\,^1A_1(n\rightarrow 3p_y)$	7.17	7.12	0.016	186	−1.842
$5\,^1B_2(\pi\rightarrow\pi^*)$	8.34	7.16	0.085	107	−3.368
$3\,^1A_2(n\rightarrow 3p_x)$	6.99	7.31	forb.	188	−1.281
$7\,^1A_1(\pi\rightarrow\pi^*)$	8.81	7.36	0.340	113	−3.175
$4\,^1A_2(n\pi\rightarrow\pi^*\pi^*)$[c]	8.25	7.39	forb.	95	−1.073
$6\,^1B_2(n\rightarrow 3p_z)$	6.80	7.40	0.003	213	9.457
$4\,^1B_1(n\rightarrow\pi^*)$	7.97	7.51	0.000	96	−1.067
$5\,^1A_2(\pi\rightarrow 3s)$	7.89	7.96	forb.	162	2.092
$1\,^3B_2(\pi\rightarrow\pi^*)$	1.50	2.75	⋯	105	−3.328
$1\,^3A_2(n\rightarrow\pi^*)$	3.77	3.74	⋯	95	−1.052
$1\,^3A_1(\pi\rightarrow\pi^*)$	2.89	3.77	⋯	104	−2.908
$1\,^3B_1(n\pi\rightarrow\pi^*\pi^*)$	3.97	4.05	⋯	95	−0.205

[a]PMCAS-CI wave functions. See Methods.
[b]Labels ($\pi\pi\rightarrow\pi^*\pi^*$) or ($n\pi\rightarrow\pi^*\pi^*$) describe states with predominant double excited character.
[c]Due to intruder state problems a level-shift of 0.4 a.u. was used in this state.

TABLE VI. Computed CASSCF (CAS), PMCAS-CI, and MS-CASPT2 (MSPT2) excitation energies (eV), oscillator strengths (f), orbital extensions ($\langle r^2 \rangle$, a.u.), and dipole moments (μ, D) of the excited states and electronic transitions of the cycloheptatrienethione (C_7H_6S) molecule.

			PMCAS-CI[a]		
State[b]	CAS	MSPT2	f	$\langle r^2 \rangle$	μ
$1\,^1A_1$				111	−4.210
$1\,^1A_2(n\rightarrow\pi^*)$	2.22	2.05	forb.	110	−1.660
$1\,^1B_1(n\rightarrow\pi^*)$	2.78	2.10	0.000	112	0.451
$1\,^1B_2(\pi\rightarrow\pi^*)$	2.95	2.31	0.027	115	−1.663
$2\,^1A_1(\pi\rightarrow\pi^*)$	4.11	3.21	0.598	112	−7.275
$3\,^1A_1(\pi\rightarrow\pi^*)$	5.67	4.74	0.037	115	−4.989
$2\,^1B_2(\pi\pi\rightarrow\pi^*\pi^*)$	5.81	4.80	0.073	118	−1.951
$3\,^1B_2(\pi\rightarrow\pi^*)$	6.17	5.19	0.092	110	−8.208
$4\,^1A_1(\pi\pi\rightarrow\pi^*\pi^*)$	5.79	5.22	0.147	115	−2.420
$4\,^1B_2(n\rightarrow 3s)$	5.00	5.23	0.019	178	2.201
$2\,^1B_1(\pi\rightarrow 3s)$	5.12	5.32	0.002	178	3.251
$2\,^1A_2(n\pi\rightarrow\pi^*\pi^*)$	5.98	5.44	forb.	116	−0.680
$5\,^1A_1(n\rightarrow 3p_y)$	5.45	5.47	0.004	263	0.614
$3\,^1B_1(n\pi\rightarrow\pi^*\pi^*)$	6.46	5.78	0.000	114	−0.581
$5\,^1B_2(n\rightarrow 3p_z)$	5.49	5.82	0.016	185	1.142
$6\,^1B_2(\pi\rightarrow\pi^*)$	7.09	5.87	0.025	115	−2.174
$3\,^1A_2(n\rightarrow 3p_x)$	5.51	5.91	forb.	217	1.215
$6\,^1A_1(\pi\rightarrow 3p_x)$	5.58	5.95	0.006	242	1.651
$4\,^1A_2(\pi\rightarrow 3p_y)$	5.67	5.97	forb.	271	2.378
$7\,^1A_1(\pi\rightarrow\pi^*)$	7.69	6.04	0.068	115	−1.939
$4\,^1B_1(\pi\rightarrow 3p_z)$	5.77	6.09	0.000	191	3.764
$5\,^1A_2(n\pi\rightarrow\pi^*\pi^*)$	8.05	6.19	forb.	114	−0.051
$5\,^1B_1(n\pi\rightarrow\pi^*\pi^*)$	7.78	6.28	0.000	109	−1.036
$6\,^1A_2(n\pi\rightarrow\pi^*\pi^*)$	7.07	6.35	forb.	111	−1.982
$6\,^1B_1(n\pi\rightarrow\pi^*\pi^*)$	7.24	6.40	0.000	111	−0.648
$7\,^1B_2(\pi\rightarrow\pi^*)$[c]	8.13	7.14	0.097	117	−4.194
$8\,^1A_1(\pi\rightarrow\pi^*)$	7.89	7.15	0.009	115	−4.916
$8\,^1B_2(\pi\rightarrow\pi^*)$	8.58	7.33	0.169	115	−3.866
$7\,^1A_2(\pi\rightarrow 3s)$	7.91	7.66	forb.	183	−0.199
$7\,^1B_1(\pi\rightarrow 3s)$	7.65	7.69	0.002	181	2.655
$1\,^3B_2(\pi\rightarrow\pi^*)$	1.58	2.00	⋯	118	−2.417
$1\,^3A_1(\pi\rightarrow\pi^*)$	1.78	2.11	⋯	118	−2.568
$1\,^3A_2(n\rightarrow\pi^*)$	2.10	2.15	⋯	112	−1.079
$1\,^3B_1(n\rightarrow\pi^*)$	2.65	2.48	⋯	112	−0.685

[a]PMCAS-CI wave functions. See Methods.

[b]Labels ($\pi\pi\rightarrow\pi^*\pi^*$) or ($n\pi\rightarrow\pi^*\pi^*$) describe states with predominant double excited character.

[c]Due to intruder state problems a level-shift of 0.4 a.u. was used in this state.

C_5H_4O to have a maximum at 5.67 eV with an oscillator strength of 0.280. This transition is responsible for the medium intensity peak observed at 5.56 eV with an oscillator strength 0.37. More questionable is the assignment of the broadband located at 6.9 eV. It most likely can be assigned to the $\pi\rightarrow\pi^*$ transition to the $5\,^1B_2$ state at 7.16 eV. The latter is the most intense transition computed for that range of energies, having an oscillator strength of 0.086. However, contributions from the $\pi\rightarrow 3p$ Rydberg transitions and some other weak $\pi\rightarrow\pi^*$ band cannot be ruled out. Finally, the region of the spectrum above 7.2 eV is clearly dominated by the transition to the $7\,^1A_1$ state, computed at 7.36 eV with an oscillator strength of 0.340. The presence of this transition explains the intense band observed in the experimental vapor spectrum.[21]

The computed spectrum of cycloheptatrienethione (C_7H_6S) has a structure similar to that of tropone. Apart from the already mentioned $n\rightarrow\pi^*$ excitations, the lowest $\pi\rightarrow\pi^*$ transition computed at 2.31 eV with an oscillator strength of 0.027 can possibly be related to the weak peak observed at 2.03 eV in the hexane spectrum.[23] The most intense band which has been recorded experimentally is located at 3.34 eV in hexane with an extinction coefficient of $15\,135\,\mathrm{l\,mol^{-1}\,cm^{-1}}$ and at 3.25 eV in methanol.[23] The assignment to the $2\,^1A_1$ state computed at 3.21 eV with an oscillator strength of 0.598 is straightforward. The batochromic shift of about 0.1 eV in polar solvents is consistent with the large dipole moment of the $2\,^1A_1$ state. Two less intense bands are reported at 4.90 and 5.53 eV with extinction coefficients 9338 and $7762\,\mathrm{l\,mol^{-1}\,cm^{-1}}$, respectively, in both hexane and methanol.[23] Their assignment is less clear. A number of $\pi\rightarrow\pi^*$ transitions in that region may contribute to the intensity of the 4.90 eV band. The most likely candidates are $3\,^1A_1$ at 4.74 eV ($f=0.037$), $2\,^1B_2$ at 4.80 eV ($f=0.073$), $2\,^1B_2$ at 5.19 eV ($f=0.092$), and, particularly $4\,^1A_1$ at 5.22 eV ($f=0.147$). The analysis of the CASSCF wave function of the $4\,^1A_1$ state indicates that this state also contains a large contribution from doubly excited configurations. In view of the structure of the wave function the large oscillator strength is somewhat surprising. Another weak band has been observed at 5.53 eV in the spectrum of C_7H_6S in both hexane and methanol. Assuming that no Rydberg transition contributes to the intensity in condensed media, the shoulder can be most probably attributed to the transition to the $5\,^1B_2$ state, computed at 5.87 eV with an oscillator strength of 0.025. However, a contribution of the lower energy $4\,^1A_1$ band cannot be discarded. To our knowledge, there is no experimental study of the electronic spectrum of C_7H_6S investigating the energy region beyond 6.0 eV. The most prominent transition in this energy range is the excitation to the $7\,^1B_2$ state, computed at 7.33 eV, with an oscillator strength of 0.169.

E. The spectra of the cross-conjugated cyclic hydrocarbons

Before confronting the spectroscopic properties of the cyclic ketones and thioketones with those of the cross-conjugated cyclic hydrocarbons, it is useful to recall the standard model of the electronic structure of such molecules.[1,2] The three and seven-carbon ring systems are known to have a strong charge donor character. In contrast, the five-membered ring is largely an electron attractor. This is clearly seen from the stability of their radicals cations and anions, respectively.[24] The basic trends observed in the excitation energies on passing from the small to the large rings are therefore well explained: In general, a decrease of the transition energies is observed, for the lowest $n\rightarrow\pi^*$ and $\pi\rightarrow\pi^*$ excitations when passing from the three- to five-membered ring compounds. This trend can undoubtedly be related to the electron attractor character of the five-carbon cycle. In contrast, and in accordance with the electron donor nature of the seven-membered ring system, an increase of the excitation energies is observed for these systems as compared to the five-membered ring compounds. Table VII compiles the computed and experimental data for the spectrum of the discussed compounds. Two factors determine the excited states properties of the heterosubstituted compounds with

TABLE VII. Computed (MS-CASPT2 unless indicated) and experimental excitation energies (ΔE, eV) and oscillator strengths (f) for the compounds shown in Fig. 1.

State	CASPT2 ΔE	CASPT2 f	Expt. ΔE (f)	MSCASPT2 ΔE	MSCASPT2 f	Expt. ΔE (f)	MSCASPT2 ΔE	MSCASPT2 f	Expt. ΔE (f)
	C_4H_4[a]			C_3H_2O[b]			C_3H_2S		
$n\rightarrow\pi^*$	···	···	···	4.25	0.001	4.13 (0.005)	3.23	forb.	···
$n\rightarrow\pi^*$	···	···	···	5.59	forb.	5.5 (0.03)	3.47	0.000	···
$\pi\rightarrow\pi^*$	4.13	0.009	4.01 (0.01)	5.96	0.116	6.1 (0.20)	4.34	0.028	···
$\pi\rightarrow\pi^*$	6.82	0.584	6.02 (0.34)	7.80	0.653	7.9–8.1 (0.65)	5.52	0.533	···
	C_6H_6[c]			C_5H_4O[d]			C_5H_4S		
$n\rightarrow\pi^*$	···	···	···	2.48	forb.	···	1.43	forb.	···
$n\rightarrow\pi^*$	···	···	···	4.49	0.000	···	2.89	0.000	···
$\pi\rightarrow\pi^*$	3.29	0.005	3.34 (0.01)	3.00	0.045	3.27 (79)	1.99	0.002	···
$\pi\rightarrow\pi^*$	5.30	0.060	5.27 (0.34)	5.42	0.097	···	4.42	0.368	···
$\pi\rightarrow\pi^*$	5.75	0.248		5.98	0.259	6.21 (55000)	4.84	0.000	···
$\pi\rightarrow\pi^*$	···	···	···	7.10	0.384	···	5.06	0.050	···
	C_8H_8[e]			C_7H_6O[f]			C_7H_6S[g]		
$n\rightarrow\pi^*$	···	···	···	3.86	0.000		2.05	forb.	1.82 (9)
$n\rightarrow\pi^*$	···	···	2.91 (0.02)	3.94	forb.	4.13 (0.13)	2.10	0.000	2.03 (47)
$\pi\rightarrow\pi^*$	···	···	4.43 (0.39)	4.22	0.064		2.31	0.027	
$\pi\rightarrow\pi^*$	···	···	···	4.26	0.042		···	···	···
$\pi\rightarrow\pi^*$	···	···	5.82 (0.5)	5.67	0.280	5.56 (0.37)	3.21	0.598	3.34 (15135)
$\pi\rightarrow\pi^*$	···	···	···	···	···	···	4.74	0.037	4.90 (9332)
$\pi\rightarrow\pi^*$	···	···	···	6.05	0.012	···	4.80	0.073	
$\pi\rightarrow\pi^*$	···	···	···	6.31	0.055	···	5.19	0.092	5.53 (7762)
$\pi\rightarrow\pi^*$	···	···	···	7.05	0.000	6.9 (0.1)	5.22	0.147	
$\pi\rightarrow\pi^*$	···	···	···	7.16	0.086		5.87	0.025	
$\pi\rightarrow\pi^*$	···	···	···	···	···	···	7.14	0.097	···
$\pi\rightarrow\pi^*$	···	···	···	···	···	···	7.15	0.009	···
$\pi\rightarrow\pi^*$	···	···	···	7.36	0.340	>7.2	7.33	0.169	···

[a]CASPT2 (Ref. 30). Spectrum in *n*-pentane (Ref. 31).
[b]Electron impact spectrum (Ref. 18). See also Ref. 32. Intensities as band heights normalized to 0.65.
[c]CASPT2 (Ref. 33). Electron-energy-loss spectrum (Ref. 33). See also Ref. 34.
[d]Optical absorption spectrum (Ref. 20). Intensities as extinction coefficients ($l\,mol^{-1}\,cm^{-1}$).
[e]Optical absorption spectrum (Ref. 35). See also Ref. 21.
[f]Vapor spectra (Refs. 21, 36). See also Ref. 37.
[g]Spectrum in hexane (Refs. 23, 38). See also Ref. 39. Intensities as extinction coefficients ($l\,mol^{-1}\,cm^{-1}$).

identical rings: The electron affinity of the heteroatom (higher for the oxygen) and the length of the exocyclic double bond (larger in the sulfur compounds). Within the family of systems with a cyclopropene ring, it is more favorable to transfer charge from the lone pair to the ring in C_3H_2S than in C_3H_2O. The excitation towards the C═S antibonding orbital is more favorable due to the relaxation of the C═S bond, as it is reflected by the decrease in the excitation energy for the $1\,^1B_1$ $n\rightarrow\pi^*$ transition in C_3H_2S with respect to C_3H_2O. The electron affinity of the exocyclic heteroatom works in the opposite direction. The two lowest $\pi\rightarrow\pi$ excited valence states of methylenecyclopropene (C_4H_4) are placed at lower energies than the corresponding states of cyclopropenone. The blue shift amounts to about 1.8 and 1.0 eV for the first and second lowest $\pi\rightarrow\pi$ excited valence state, respectively. Changing the oxygen atom by a sulfur atom leads again to a redshift. It is interesting to note that it is larger for the second lowest $\pi\rightarrow\pi$ excited valence state (1.6 vs 2.3 eV). The strong electron attractor character of oxygen is responsible for such behavior.

A completely different trend is observed for the substituted cyclopentadiene systems. In these systems the five-membered ring is strongly competing with the electron affinity of the exocyclic heteroatom. This leads, in general, to a drop of the transition energies. As can be expected this effect is smallest for fulvene and largest for C_5H_4O (a decrease of 2.96 eV for the first $\pi\rightarrow\pi^*$ excited valence state). Finally, for the seven-membered ring compounds the trend is reverted due to the electron donor character of the ring. Despite the changes in the position of the low-lying states, it can be observed that, in general, the bulk of the intensity goes in all cases into a transition to a $^1A_1$ excited state, whose excitation energy drops by around 1 eV with each step the size of the ring is increased.

F. The NLO properties of the cyclic ketones and thioketones

The specific excited state structure of ketones and thioketones, in particular their low excitation energies and large intensities, makes them special subjects of interest from the point of view of materials with nonlinear optical (NLO)

properties.[5,6] Recently we presented a study[5] of the NLO properties of cyclic ketones and thioketones. We focused on the static electric properties ranging from dipole moments to third order polarizabilities. From the knowledge of the excited state properties such as excitation energies and transition dipole moments a number of NLO properties can be obtained by means of perturbative techniques known as the sum-over-states (SOS) method.[25,26] We think that this give us the opportunity to complement the previous study on excited states of ketones and thioketones with an analysis of the main contributions to the NLO properties. Here we shall compare some of the molecular properties obtained by applying SOS methods with the results obtained earlier using finite-field *ab initio* calculations.[5] In particular, we shall analyze the *zz*- and *zzz*-components of the polarizability (α_{zz}) and first hyperpolarizability (β_{zzz}) using a two- (SOS2) and three-level (SOS3) sum-over-states procedure.[27] We will restrict the analysis to the contributions of the valence $\pi \rightarrow \pi^*$ transitions. This study should not be considered a test of the SOS possibilities. Our main goal is to use accurate spectroscopical data to analyze the contributions to the NLO properties by using the SOS method.

To compute the components of the polarizability tensors we applied following formulas which were obtained from perturbation theory:[28]

$$\alpha = \sum_I \frac{M_{gI}^2}{\Delta E_{gI}}, \tag{1}$$

where M_{gI} is the transition dipole moment between the ground state g and the excited state I and ΔE_{gI} is the corresponding excitation energy. Two different models have been considered to compute the first hyperpolarizability, β. The expression of the two-state sum-of-states model (SOS2) can be written as[27]

$$\beta_{\mathrm{SOS2}} = \sum_I \frac{M_{gI}^2 \Delta \mu_{gI}}{\Delta E_{gI}^2}. \tag{2}$$

It includes the transition dipole moments M_{gI}, the energy differences ΔE_{gI}, and the elements $\Delta \mu_{gI}$. The latter correspond to the difference between the ground and excited state dipole moments. The summation can be reduced to one single term when the system has a clear dominant transition and charge transfer is unidirectional, as it is in the case of typical organic chromophores. The two-state model is then reduced to the classical Oudar expression.[29] The three-level SOS model involves the ground and two excited states, I and J,

$$\beta_{\mathrm{SOS3}} = \sum_I \sum_{J \neq I} \frac{M_{gI} M_{gJ} M_{IJ}}{\Delta E_{gI} \Delta E_{gJ}}. \tag{3}$$

In the following discussion we shall focus only on the α_{zz} and β_{zzz} components of the polarizability tensors. For symmetry reasons only states of $^1A_1$ symmetry contribute to these elements.

TABLE VIII. Main elements contributing to the two-level SOS expression in the computed molecules.

Molecule	State	ΔE_{gi} (eV)	f	$-\Delta \mu_{gi}$ (D)
C_3H_2O	$4\ ^1A_1$	7.80	0.653	−0.881
C_3H_2S	$2\ ^1A_1$	5.52	0.533	−0.488
C_5H_4O	$3\ ^1A_1$	5.98	0.259	0.492
	$5\ ^1A_1$	7.10	0.384	−0.889
C_5H_4S	$2\ ^1A_1$	4.42	0.368	1.279
C_7H_6O	$3\ ^1A_1$	5.67	0.280	0.785
	$7\ ^1A_1$	7.36	0.340	−0.566
C_7H_6S	$2\ ^1A_1$	3.21	0.598	3.065
	$4\ ^1A_1$	5.22	0.147	−1.790

In the following discussion we shall focus only on the α_{zz} and β_{zzz} components of the polarizability tensors. For symmetry reasons only states of $^1A_1$ symmetry contribute to these elements.

Table VIII compiles the electronic properties of the most important states for the different systems which enter the SOS2 formula of β_{zzz}. The same states have been selected to contribute to the SOS3 expression, although the corresponding transition dipole moment elements are listed as auxiliary material.[17] Table IX lists the values of α_{zz} and β_{zzz} obtained for the different systems, both at the SOS2, SOS3, and finite-field levels. The results show the well known weakness of the SOS model: It is very sensitive to the proper choice of states included in the expansion. Unless there is a well-defined electronic transition which combines a large intensity with a strong charge transfer character, the obtained results,

TABLE IX. Components of the polarizability and first hyperpolarizability tensor of the studied ketones and thioketones at different levels of theory (a.u.).[a,b]

Comp.	SOS2	SOS3	MP2	CASPT2	SOS2	SOS3	MP2	CASPT2
	C_3H_2O				C_3H_2S			
α_{zz}	11.92	⋯	48.34	47.75	19.41	⋯	84.33	82.70
β_{zzz}	13.59	⋯	52.89	67.64	18.38	⋯	−12.43	−59.21
	C_5H_4O				C_5H_4S			
α_{zz}	24.92	⋯	76.11	75.40	20.81	⋯	116.36	113.96
β_{zzz}	1.00	20.89	26.12	38.31	−44.08	−74.87	−403.57	−197.93
	C_7H_6O				C_7H_6S			
α_{zz}	56.04	⋯	121.99	120.27	74.64	⋯	188.72	185.11
β_{zzz}	−44.57	−119.67	−159.44	−181.88	−633.22	−680.87	−1203.86	−1666.44

[a]Two (SOS2) and three (SOS3) levels sum-over-states method. See text.
[b]Finite-field MP2 and CASPT2 calculations (Ref. 5).

although showing often the right trends, are unlikely to produce quantitatively correct data. We have decided to focus in the α_{zz} and β_{zzz} components, only, because of the bulk of the intensity in the computed molecules is obtained by states of $^1A_1$ symmetry, and therefore the application of SOS methods is justified. The finite-field results show a change in sign and a increase β_{zzz} on enlarging the molecular size for the oxo-substituted systems, while a large increase in negative values is observed for the sulfur-substituted compounds. The SOS values fall within the right order of magnitude. In all cases, however, the values of α_{zz} and β_{zzz} are about half of the value computed with the finite-field approach.[5] The trends are therefore correct, and, except for cyclopropenethione, the components have the right sign. The systematic underestimation of the tensor elements is basically related to the fact that the transitions have no strong charge transfer character. If one considers other components, such as β_{xxz}, involving transitions to states of $^1B_1$ symmetry, the SOS results largely underestimate the finite-field values because of the very small transition dipole moment values. This clearly shows, that the model cannot provide accurate results unless a much larger number of states is considered. In some of the cases the use of the three-level model, has noticeable consequences in the final results, an indication of the important contributions of transition dipole moments between the different excited states.[17]

The simplicity of the SOS model, however, allows to analyze the trends in terms of the excited states and transition properties and also allows to explain the irregularity we find for cyclopropenethione. Table VIII compiles the electronic properties of the most important states for the different systems which enter the SOS2 formula of β_{zzz}. For the three-membered ring compounds the summation reduces to a single term. Therefore, the sign of β_{zzz} is determined by the sign of $\Delta\mu_z$. By inspection of Table VIII we find that the $^1A_1$ excited state dipole moments of the cyclopropeneketones decreases with respect to the ground state values leading, in both cases, to a positive contribution to β_{zzz}. Therefore, the two-level model cannot account for the negative value of the component in C_3H_2S.

The increase of β_{zzz} components on increasing the molecular size can also be understood from the data shown in Table VIII. On going from the three- to the five-membered ring compounds, a large decrease of the excitation energies is observed, which combined with a reversal on the excited states dipole moment change leads to the increase of β_{zzz}. The change in the excited state dipole moment is particularly large (1.279 D) in cyclopentadienethione. In contrast, the change of intensity of the corresponding electronic transitions is small. Therefore we find a large decrease in the β_{zzz} component, whereas α_{zz} is hardly changed. As regards the C_5H_4O the situation is different. β_{zzz} includes two contributions with dipole moment changes of opposite sign. Hence, the overall effect is rather small. Enlarging the ring towards the cycloheptatriene-type structure causes β_{zzz} to dramatically increase. The excitation energies and transition intensities do not change drastically. The largest differences are found for the low-lying $^1A_1$ excited state dipole moments, which reflect the electron donor–acceptor properties of the different ring systems. As discussed in previous section the five-membered ring accepts charges whereas the three- and seven-membered rings are charge donors. Especially in thiotropone the combination of low excitation energies, large transition intensities, and large dipole moment for the $2\,^1A_1$ $\pi\pi^*$ state leads to a very large value of the first hyperpolarizability component.

Finally, we may conclude that in order to maximize the NLO properties of a compound research has to focus on low lying intense electronic transitions. In addition, chemical modification should be made in such ways to maximize the difference in dipole moments of ground and excited states where as the overall volume of the compound should change as little as possible. For the present systems, the substitution of oxygen by sulfur leads to a decrease in the excitation energies. In addition, the transfer of charge from the ring to the heteroatom is easier because of the longer C═S bond and the lower electron affinity of the sulfur compared to oxygen. This leads to the desired large increase in the dipole moment differences for the low-lying $^1A_1$ and also $^1B_2$ states.

IV. SUMMARY AND CONCLUSIONS

The electronic absorption spectra of a series of exocyclic ketones and thioketones have been studied by means of the CASSCF/MS-CASPT2 approach. State energies and transition properties of a large number of valence and Rydberg, singlet, and triplet excited states have been included in the study. The discussion focused on the characteristics of the spectra and the relation among the different states upon substitution of the exocyclic double bond has been performed. Comprehensive and sometimes novel assignments of the observed bands have been proposed for most of the compounds.

Particular attention has been given to the calculation of transition matrix elements between the different electronic states. This information has been used to analyze the contributions to the NLO properties because of the potential use of these molecules in the synthesis of novel materials. The NLO properties were compared to results obtained earlier using the *finite field* approach. A perturbative approach, the SOS approach, has been used to estimate NLO properties from spectroscopic data. If restricted to a small number of states, the method has been found to give qualitatively correct results which reproduce the trends but underestimate the absolute values. The key of the study is, however, that the SOS method allows a detailed analysis of the main effects related to the excited states structure contributing to the NLO molecular properties.

ACKNOWLEDGMENTS

The authors acknowledge the financial support obtained by the TMR Network DELOS, Contract No. FMRX-CT96-0047, by a grant from the Swedish Natural Science Research Council (NFR), by Project Nos. PB97-1377 and BQU2001-2926 of Spain, and by the Generalitat Valenciana. The support by the CNPq (Conselho Nacional de Desenvolvimento Científico Tecnológico) and FAPESP (Fundação de Amparo

à Pesquisa do Estado de São Paulo) is acknowledged. The authors also thank Professor A. J. Sadlej for fruitful suggestions and comments. L.S.A. acknowledges a project in the program 'Ramon y Cajal' from the MCYT.

[1] G. Buemi, F. Zuccarello, and A. Raudino, J. Mol. Struct.: THEOCHEM **76**, 137 (1981).
[2] D. Lloyd, *The Chemistry of Conjugated Cyclic Compounds* (Wiley, New York, 1990).
[3] P. J. Domaille, J. E. Kent, and M. F. O'Dwyer, Chem. Phys. **6**, 66 (1974).
[4] T. Pluta and A. J. Sadlej, J. Chem. Phys. **114**, 136 (2001).
[5] U. Eckart, L. Serrano-Andrés, M. P. Fülscher, and A. J. Sadlej, J. Chem. Phys. **113**, 6235 (2000).
[6] J. Mizuguchi, T. Suzuki, S. Matsumoto, and H. Otani, J. Phys. Chem. B **103**, 426 (1999).
[7] B. O. Roos, K. Andersson, M. P. Fülscher, L. Serrano-Andrés, K. Pierloot, M. Merchán, and V. Molina, J. Mol. Struct.: THEOCHEM **388**, 257 (1996).
[8] J. P. Finley, J. Chem. Phys. **108**, 1081 (1998).
[9] B. O. Roos, K. Andersson, M. P. Fülscher, P.-Å. Malmqvist, L. Serrano-Andrés, K. Pierloot, and M. Merchán, in *Advances in Chemical Physics: New Methods in Computational Quantum Mechanics*, edited by I. Prigogine and S. A. Rice (Wiley, New York, 1996), Vol. XCIII, pp. 219–231.
[10] J. Finley, P.-Å. Malmqvist, B. O. Roos, and L. Serrano-Andrés, Chem. Phys. Lett. **288**, 299 (1998).
[11] M. Merchán, L. Serrano-Andrés, M. P. Fülscher, and B. O. Roos, in *Recent Advances in Multireference Theory*, edited by K. Hirao (World Scientific, Singapore, 1999), Vol. IV, pp. 161–195.
[12] P.-O. Widmark, P.-Å. Malmqvist, and B. O. Roos, Theor. Chim. Acta **77**, 291 (1990).
[13] P.-O. Widmark, B. J. Persson, and B. O. Roos, Theor. Chim. Acta **79**, 419 (1991).
[14] B. O. Roos, M. P. Fülscher, Per-Åke Malmqvist, M. Merchán, and L. Serrano-Andrés, in *Quantum Mechanical Electronic Structure Calculations with Chemical Accuracy*, edited by S. R. Langhoff (Kluwer Academic, The Netherlands, 1995), pp. 357–438.
[15] P. Å. Malmqvist and B. O. Roos, Chem. Phys. Lett. **155**, 189 (1989).
[16] K. Andersson, M. R. A. Blomberg, M. P. Fülscher *et al.*, MOLCAS, Version 4.1, Department of Theoretical Chemistry, Chemistry Center, University of Lund, Lund, Sweden, 1999.
[17] See EPAPS Document No. E-JCPSA6-117-305226 including the full CASSCF, PMCAS-CI, CASPT2, and MS-CASPT2 excited state properties of the six studied cyclic ketones and thioketones, and the computed PMCAS-CI transition dipole moments among the respective valence states. This document may be retrieved via the EPAPS homepage (http://www.aip.org/pubservs/epaps.html) or from ftp.aip.org in the directory /epaps/. See the EPAPS homepage for more information.
[18] W. R. Harshbarger, N. A. Kuebler, and M. B. Robin, J. Chem. Phys. **60**, 345 (1974).
[19] M. P. Fülscher and B. O. Roos, Theor. Chim. Acta **87**, 403 (1994).
[20] E. W. Garbisch, Jr. and R. F. Sprecher, J. Am. Chem. Soc. **88**, 3433 (1966).
[21] H. Hosoya and S. Nagakura, Theor. Chim. Acta **8**, 319 (1967).
[22] E. Weltin, E. Heilbronner, and H. Labhart, Helv. Chim. Acta **46**, 2041 (1963).
[23] T. Machiguchi, H. Otani, Y. Ishii, and T. Hasegawa, Tetrahedron Lett. **28**, 203 (1987).
[24] *The Chemistry of Heterocyclic Compounds* (Wiley-Interscience, New York, 1972–1983).
[25] J. F. Ward, Rev. Mod. Phys. **37**, 1 (1971).
[26] B. J. Orr and J. F. Ward, Mol. Phys. **20**, 513 (1971).
[27] D. R. Kanis, M. A. Ratner, and T. J. Marks, J. Am. Chem. Soc. **114**, 10338 (1992).
[28] S. A. Locknar, L. A. Peteanu, and Z. Shuai, J. Phys. Chem. A **103**, 2197 (1999).
[29] J. L. Oudar, J. Chem. Phys. **67**, 446 (1971).
[30] M. Merchán, R. González-Luque, and B. O. Roos, Theor. Chim. Acta **94**, 143 (1996).
[31] S. W. Staley and T. D. Norden, J. Am. Chem. Soc. **106**, 3699 (1984).
[32] R. Breslow and M. Oda, J. Am. Chem. Soc. **94**, 4788 (1972).
[33] K. R. Asmis, M. Allan, O. Schafer, and M. Fülscher, J. Phys. Chem. A **101**, 2089 (1997).
[34] P. A. Straub, B. Meuche, and E. Heilbronner, Helv. Chim. Acta **49**, 517 (1965).
[35] W. E. Doering and D. E. Wiley, Tetrahedron **11**, 183 (1960).
[36] H. Hosoya, J. Tanaka, and S. Nagakura, Tetrahedron **18**, 859 (1962).
[37] N. L. Bauld and Y. S. Rim, J. Am. Chem. Soc. **89**, 6763 (1967).
[38] T. Machiguchi, T. Hoshi, J. Yoshino, and Y. Kitahara, Tetrahedron Lett. **1973**, 3873.
[39] H. A. Dugger and A. S. Dreiding, Helv. Chim. Acta **59**, 747 (1976).